Linear analysis of a finite length plasma-filled backward wave oscillator

M. M. Ali, K. Ogura, and K. Minami
Graduate School of Science and Technology, Niigata University, Niigata 950-21, Japan

T. Watanabe
National Institute for Fusion Science, Nagoya 464-01, Japan

W. W. Destler and V. L. Granatstein
Laboratory for Plasma Research, University of Maryland, College Park, Maryland 20742

(Received 11 October 1990; accepted 3 January 1992)

Absolute instability in a plasma-filled backward wave oscillator with sinusoidally corrugated slow wave structure driven by an intense relativistic electron beam has been analyzed numerically. The maximum spatial growth rate of the plasma-filled waveguide is found to be larger than that of an optimally designed vacuum structure. The excitation of a finite length structure is investigated. Although the spatial growth rates obtained in the linear theory increase with plasma density in the finite length plasma-filled structure for the fundamental TM_{01} mode of oscillation, negative global spatial growth rates prevent the coherent oscillation for intermediate ranges of plasma density, beam current, and even for structure length.

I. INTRODUCTION

In recent years, extensive efforts have been devoted to finding microwave sources[1] at frequency ranges and power levels beyond the capabilities of the existing ones. In the last decade, developments in gyrotrons and free-electron lasers have made it possible to produce short wavelength radiation at modest power levels. In addition to the innovation of such wholly novel classes of microwave sources, researchers are also working to improve the performances of more familiar devices such as magnetrons and backward wave oscillators (BWO's) driven by intense relativistic electron beams (IREB's).

BWO's have a long history as efficient generators of microwave power. During the past two decades, impressive results have been obtained both experimentally and theoretically with these devices.[2-14] The use of IREB's as the source of energy for the microwaves has resulted in a tremendous increase in the output power from BWO's. The multiwave Cerenkov generator[15] and relativistic diffraction generator,[16] which have a close relationship to BWO's, attained output power levels greater than 1 GW at frequencies of tens of GHz with high efficiencies. Previously, improvements in efficiency were observed when BWO's were operated in the presence of background gases.[3,4,13] An eightfold enhancement in output power was achieved by the injection of plasma into a BWO from an external plasma gun.[14] Lin and Chen[17] reported numerical simulations of the experiment,[14] although they assumed an artificial periodic boundary condition in the axial direction which did not correspond to the experiment. They reported that a parametric beam–plasma wave interaction could not be the dominant mechanism for the efficiency enhancement and that the enhancement could be attributed to a decrease in the phase velocity of the most unstable beam mode in the presence of a background plasma.

In order to understand the elementary physics on what was happening in the plasma-filled BWO's[13,14] within the scope of linear treatment, we have here developed and analyzed numerically the absolute instability in the plasma-filled BWO's. We first consider an infinitely long plasma-filled corrugated waveguide, and next proceed to finite length case which is somewhat more complicated than the former case. Analyses are made within the general frameworks of absolute instability established in the textbook of Briggs[18] for the case of infinitely long structure, and in that of Lifshitz and Pitaevskii[19] for finite length case. Even in the case of infinitely long structure, we assume a localized source[18,19] of signals as the original perturbation. It is known that the absolute instability with this type of perturbation grows up with the particular values of complex wave number k_s and complex angular frequency ω_s at a saddle point (pinch point) of a dispersion relation in which an arbitrary set of k and ω can be conceived in general. To find the saddle points, we must solve the dispersion relation assuming k and ω both complex.[18] On the other hand, if one assumes an infinitely extending sinusoidal origin of perturbation in space, then an arbitrary real wave number k can be assumed in the analysis of the absolute instability. We do not consider, however, such a case in our analysis. This paper presents what we believe to be the first pinch point analysis of the dispersion relation of a plasma-filled BWO. It will be shown that, according to our pinch point analysis, increased spatial growth rates in the plasma BWO's[13,14] can be expected for both infinitely long and finite length structures. Of course, in general, nonlinear analyses are required to predict enhanced radiation intensities.

The organization of this paper is as follows. In Sec. II, we formulate the linear theory of an infinitely long plasma-filled BWO. The spatial and temporal growth rates of absolute instabilities for a waveguide with large corrugation depth[13,14] are calculated numerically over a wide range of plasma densities. The effects of the reflection of waves assuming a special case of mode changes at both ends of a finite length slow wave structure are analyzed in Sec. III. Finally, discussion and conclusions of this work are given in Sec. IV.

 0899-8221/92/041023-10$04.00

II. ENHANCED SPATIAL GROWTH RATES IN AN INFINITELY LONG PLASMA-FILLED BWO

A. Formulation of the problem

We consider first an infinitely long axisymmetric cylindrical waveguide, in which inner wall radius varies, according to $R(z) = R_0 + h\cos(k_0 z)$, i.e., a slow wave structure. Here $k_0 = 2\pi/z_0$ and R_0, h, and z_0 are, respectively, the mean waveguide radius, the amplitude of corrugation, and the axial length of periodicity in corrugation. The waveguide is filled completely with a uniform, cold, collisionless, and neutralized plasma of density N_p. A monoenergetic relativistic electron beam of radius $R_b < R_0 - h$, and density N_b uniform over the cross section, is moving along the axis of the waveguide with a velocity v relative to the resting background plasma. Assuming that the entire system is immersed in an infinitely strong axial guiding magnetic field, the dispersion relation, $D(k,\omega) = 0$, of this beam–plasma system for TM_{0s} modes with field components E_z, E_r, and B_θ has been derived previously.[20,21] Here, D is the value of the determinant of a square matrix with elements

$$D_{mn} = [1 + (n-m)Q_n](K_n C^J_{mn} + L_n C^N_{mn}), \quad (1)$$

$$C^J_{mn} = \sum_{q=0}^{\infty} \frac{(Y_n\alpha)^{2q+|n-m|} J_0^{(2q+|n-m|)}(Y_n)}{2^{2q+|n-m|} q!(q+|n-m|)!}, \quad (2)$$

$$K_n = Y_n J_0(X_n\delta)N_1(Y_n\delta) - X_n J_1(X_n\delta)N_0(Y_n\delta),$$

$$L_n = X_n J_0(Y_n\delta)J_1(X_n\delta) - Y_n J_0(X_n\delta)J_1(Y_n\delta),$$

$$X_n^2 = R_0^2\left(\frac{\omega^2}{c^2} - k_n^2\right)\left(1 - \frac{\omega_P^2}{\omega^2} - \frac{\omega_b^2}{\gamma^3(\omega - k_n v)^2}\right),$$

$$Y_n^2 = R_0^2\left(\frac{\omega^2}{c^2} - k_n^2\right)\left(1 - \frac{\omega_P^2}{\omega^2}\right),$$

$$Q_n = \frac{k_0 k_n}{(\omega^2/c^2) - k_n^2}, \quad \alpha = \frac{h}{R_0},$$

$$\delta = R_b/R_0, \quad k_n = k + nk_0.$$

A similar expression for C^N_{mn} holds, with J_0 replaced by N_0 in C^J_{mn} given by Eq. (2).

The beam in the structure provides the energy source to drive unstable interaction. In such an active system, the spatial growth rate may be a more practical measure of the strength of instability than the temporal growth rate for a localized perturbation source as was pointed by Briggs in Ref. 18 (p. 11).

B. Numerical solutions to the dispersion relation

In general, there exist an infinite number of roots for high frequencies in our dispersion relation. We confine our analysis to the case of the low-frequency fundamental TM_{01} mode with $\omega > \omega_p$. As was expected from previous works,[9,10,20] four independent periodic roots of TM_{01} mode with a periodicity of real wave number k_0 are found in our dispersion relation, $D(k,\omega) = 0$, in which a complex $k = k_r + ik_i$ is obtained for a given complex $\omega = \omega_r + i\omega_i$. As will be discussed later in detail, the four roots are, respectively, slow and fast beam space charge waves, forward and backward structure waves. When we depict the locations of the roots of the dispersion relation in complex k plane, we must judge ourselves whether each root corresponds to growing or decaying (stable) wave. This subtle situation arises from the fact that the principal sheet of Riemann surface of multivalued functions, for example, $\pm(X_n^2)^{1/2}$, or $\pm(Y_n^2)^{1/2}$, included in the functional equation $D(k,\omega) = 0$, is automatically chosen in the process of computer calculation without any physical consideration. So, the physical interpretation that the particular root corresponds to growing or damping wave is inevitable. For that purpose, well-known Briggs–Bers criterion[18] is applied. In order to accomplish their criterion in practice, the path of integration in the inverse Laplace transformation in the complex ω plane is deformed downward to the real axis and observe the behaviors of the corresponding roots in the complex k plane. Physical meaning of this deformation corresponds to the change from the initial value problem (large positive ω_i) to the steady-state problem ($\omega_i = 0$). According to their criterion, if k crosses the real k axis during this process, then the wave is growing, i.e., convectively unstable, otherwise, it is decaying or stable. On the other hand, if the deformation of the path of integration on the ω plane toward the real axis is prevented by merging on the complex k plane (saddle point) of two moving roots coming from the upper and lower half-planes at some positive ω_i, then the instability is absolute which corresponds to a BWO. The asymptotic time response of the absolute instability for a localized source of perturbation arises mainly from the contribution near this saddle point and not from the other parts of the integral along the real ω axis.[18] In general, ω and k at the saddle point are both complex[18,19] ($k_s = k_{rs} + ik_{is}$, $\omega_s = \omega_{rs} + i\omega_{is}$), and the absolute instability in an infinitely long structure grows up asymptotically with temporal and spatial factor $t^{-1/2}\exp[i(k_s z - \omega_s t)]$, as is shown in Eq. (2.22) in Ref. 18 or equivalently in Eq. (62.12) in Ref. 19.

In the numerical analysis presented here, the following parameters are adopted unless specified otherwise; the relativistic factor $\gamma = 2.23$, $R_b = 0.9$ cm, $R_0 = 1.445$ cm, $h = 0.445$ cm, $z_0 = 1.67$ cm, and $N_b = 2.09\times10^{11}$ cm^{-3} which corresponds to the beam current $I_b = 2.3$ kA.[13,14] The background plasma density N_p is considered to be a variable. For the assumed parameters, we must calculate the dispersion equation, $D(k,\omega) = 0$, which is here truncated to 9×9 determinant composed of each term up to the order of α^{10} in Eq. (2), to obtain the numerical accuracy in periodicity within 1% for two periods of real wave number $k_0 = 3.7624$ cm^{-1}.[20]

The method of numerical computation devised by one of the authors (T.W.) (Ref. 22) is as follows: Since the Taylor expansion of $D(k,\omega) = 0$ around the root gives an equation of a circle, the solution of k for a given complex ω can be found at the center of the contour circles of $|D|$ in the complex k plane. An example of the contour mapping devised for the present purpose is shown in Fig. 1, where $N_p = 2\times10^{12}$ cm^{-3}, $N_b = 5.15\times10^{10}$ cm^{-3}, and $\omega/2\pi = (14.65 + i\,0.04)$ GHz. The size of the white heart-shaped part

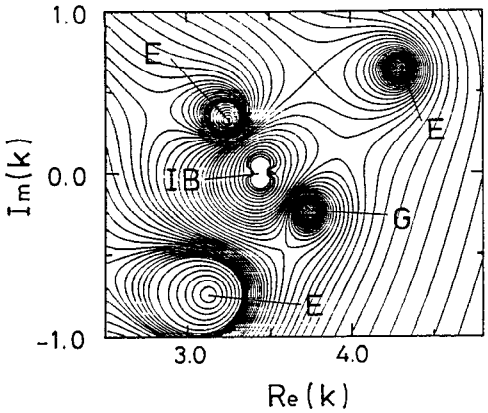

FIG. 1. Contour mapping of absolute value of D for $N_p = 2\times10^{12}$ cm^{-3}, $N_b = 5.15\times10^{10}$ cm^{-3}, and $\omega/2\pi = (14.65 + i\,0.04)$ GHz.

shown by IB (an iceberg floating on the sea) located around $\omega = k_n v$ near the real k axis increases with N_b. In IB, $|D|$ is extremely large of the order of 10^{30} or more. In other parts in Fig. 1, the values of $|D|$ are much smaller than those in IB. IB is comparatively immobile and the observed four roots move around it quickly, when ω_i is decreased toward zero from a large positive value keeping ω_r constant. The roots corresponding to decaying and growing waves are denoted, respectively, by E and G, which are judged from the Briggs–Bers criterion. These four roots appear in the complex k plane with a period of real wave number k_0, as is expected from Floquet theorem.

Taking the roots in Fig. 1 as a key to the initial data for our analysis, a Newton iteration method[22] for complex ω and k is devised to find successive changes in the loci of the roots of the dispersion relation, when ω_i is changed gradually. An example of the variation of the loci of the roots in the complex k plane is shown in Fig. 2. Thin solid and dashed lines are, respectively, the constant $\omega_r/2\pi$ and $\omega_i/2\pi$ lines. Arrows on the solid lines show the decreasing direction of ω_i's toward $\omega_i = 0$ which are marked by open circles. The roots which cross the real k axis for some $\omega_i > 0$ correspond to the spatially growing waves. The diamond in the figure indicates the saddle point which corresponds to the absolute instability in the infinitely long plasma BWO. The thick solid line passing through the saddle point with constant real frequency, $\omega_{rs}/2\pi$, separates the growing roots from decaying roots near the saddle point, and the thick solid line is called here the separatrix. The definition of the separatrix is as follows. The roots of our dispersion relation are divided into two classes: The first is the waves carrying energy in positive z direction (positive group velocity), and the second is those carrying energy in negative z direction (negative group velocity). The first and the second classes are located, respectively, above and below the separatrix. This situation comes from the inverse Fourier transformation in the complex k plane. In the first (second) class, integration along an infinitely large semicircle must be executed to close the Fourier contour in the upper-half (lower-half) k plane

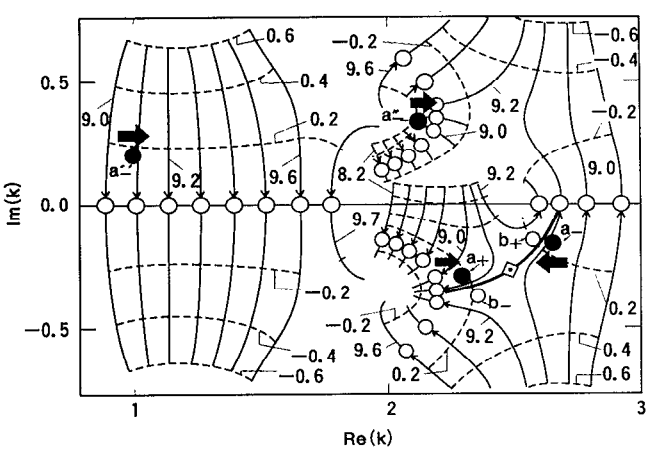

FIG. 2. Loci of the roots of the dispersion equation on the complex k plane. $N_p = 2\times10^{11}$ cm^{-3} and $I_b = 2.3$ kA. The solid and dashed lines correspond, respectively, to constant real and imaginary frequencies. Only the solid lines, which cross the Re(k) axis as ω_i decreases toward zero, correspond to the growing roots. The diamond indicates the saddle point and the open circles indicate k for real frequencies ($\omega_i = 0$). The thick solid line through the saddle point with constant real frequency, $\omega_{rs}/2\pi$, is the separatrix which separates the growing roots from those corresponding to decaying waves. See the text for thick arrows, solid and open circles denoted by a_+, a_-, a'_-, a''_-, b_+, and b_-.

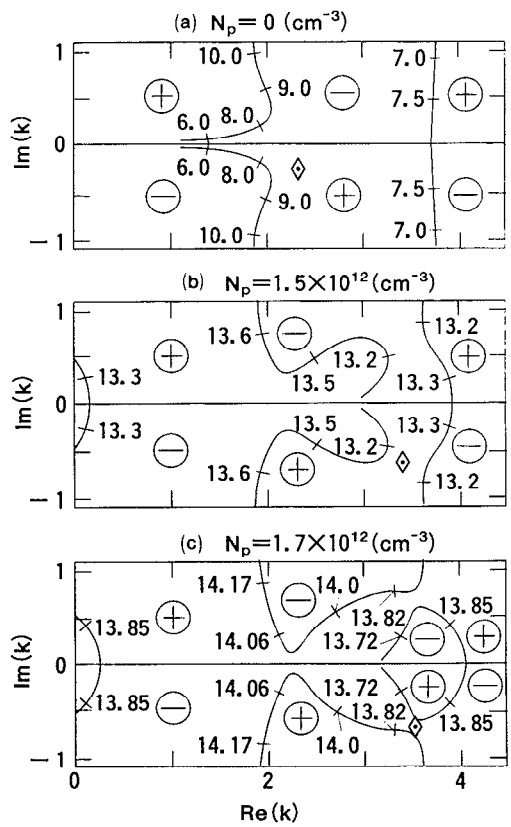

FIG. 3. Roots of the dispersion relation for real frequency on the complex k plane are shown by solid curves; (a) $N_p = 0$; (b) $N_p = 1.5\times10^{12}$ cm^{-3}; (c) $N_p = 1.7\times10^{12}$ cm^{-3}. In all cases $N_b = 2.09\times10^{11}$ cm^{-3} ($I_b = 2.3$ kA). The diamonds in ⊕ regions indicate the saddle points which correspond to the absolute instability in an infinitely long plasma-filled slow wave structure.

where the roots k are originally located for large positive ω_i. The roots marked by a_+, a_-, a'_-, a''_-, b_+, and b_- will be discussed later in Secs. III and IV.

In Fig. 3, the loci of the roots k of the dispersion relation in the complex k plane for real $\omega/2\pi$ (depicted on the curves) in the vicinity of beam-structure resonance are shown. Figures 3(a), 3(b), and 3(c) are, respectively, for $N_p = 0$, 1.5×10^{12} cm^{-3}, and 1.7×10^{12} cm^{-3}. The curves in the figures are periodic in the horizontal axis with periodicity of k_0, and they are symmetric regarding the real k axis. The regions where one finds the complex k roots of the dispersion equation for a given complex ω with $\omega_i > 0$ and $\omega_i < 0$ are marked, respectively, by $\oplus$ and $\ominus$. The absolute instability can exist only when the saddle point is located in $\oplus$ regions. The figures depict that the background plasma strongly deforms the curves near the real k axis, and pushes them to the right with increase in N_p. The saddle points in the lower half of the complex k plane are marked by the diamonds. In the cases of vacuum or low N_p, the saddle point lies in the region of $\omega_i > 0$ and $k_i < 0$ as shown in Figs. 3(a) and 3(b). The instability is, therefore, absolute. The instability, however, becomes convective as ω_{is} of the saddle point switches sign, when N_p is exceedingly large. This case of $N_p = 1.7\times10^{12}$ cm^{-3} is shown in Fig. 3(c) which corresponds to a plasma traveling wave tube (TWT). Here, the saddle point obtained mathematically has no meaning in physical point of view. The convective instability in this case cannot cause any coherent radiation unless an external positive feedback mechanism is devised.

The spatial growth rate, k_{is}, and the real part, k_{rs}, at the saddle point versus the plasma density, N_p, are plotted in Fig. 4(a), respectively, by solid and dashed lines. As is shown in Fig. 4(a), both k_{is} and k_{rs} increase with N_p. The temporal growth rate divided by 2π, $\omega_{is}/2\pi$, and the oscillation frequency, $\omega_{rs}/2\pi$, at the saddle point versus N_p are also shown, respectively, by solid and dashed lines in Fig. 4(b). The temporal growth rate of the absolute instability, ω_{is}, decreases with N_p, and switches sign at $N_p = 1.67\times10^{12}$ cm^{-3}. The instability becomes convective above that value of N_p, and the system will work as a plasma TWT, because the wave is still growing spatially. The double open circle shown by P will be discussed later, when a vacuum BWO is analyzed in Fig. 5.

Next, we look for an optimal system parameter for increasing the spatial growth rate of a vacuum BWO ($N_p = 0$). For an infinitely long waveguide, the spatial growth rate at the saddle point is found to increase with the increase in the axial length of periodicity in corrugation, z_0. For higher values in z_0, however, the absolute instability of TM_{01} mode is suppressed and only the convective instability remains. The numerical solution of spatial growth rate at the saddle point in the case of vacuum BWO is shown in Fig. 5 for a wide range of z_0. Other parameters are the same as those in the plasma BWO shown in Fig. 4. The solid circles on the curves indicate the growth rates corresponding to $z_0 = 1.67$ cm, the experimental value.[13,14] It must be noted that the maximum spatial growth rate shown by the double open circle Q in Fig. 5 of an optimally designed vacuum BWO is considerably smaller than that shown by the double open

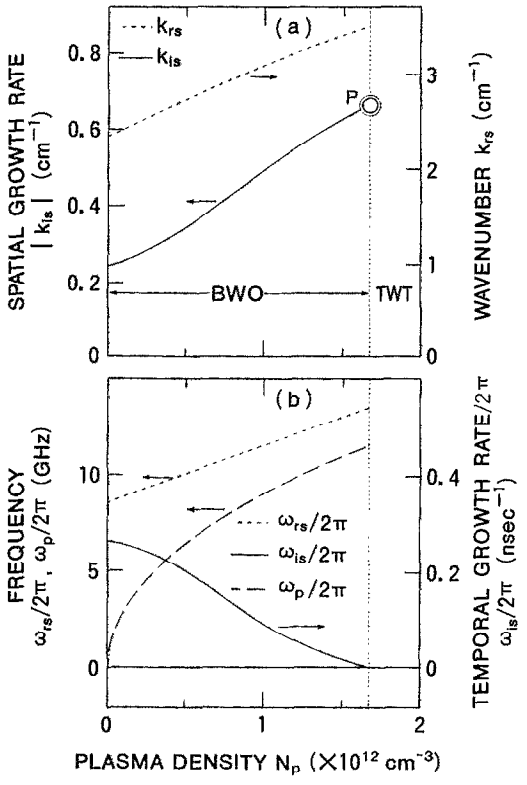

FIG. 4. Numerical solution to the dispersion relation of a plasma-loaded infinitely long slow wave structure: (a) Spatial growth rate (solid curve), k_{is}, and the real part (dashed curve), k_{rs}, at the saddle point versus plasma density N_p. (b) Temporal growth rate divided by 2π (solid curve), $\omega_{is}/2\pi$, and the oscillation frequency (dashed curve), $\omega_{rs}/2\pi$, at the saddle point, and plasma frequency (dot-dashed curve), $\omega_p/2\pi$ versus plasma density N_p. See the text for the double open circle P.

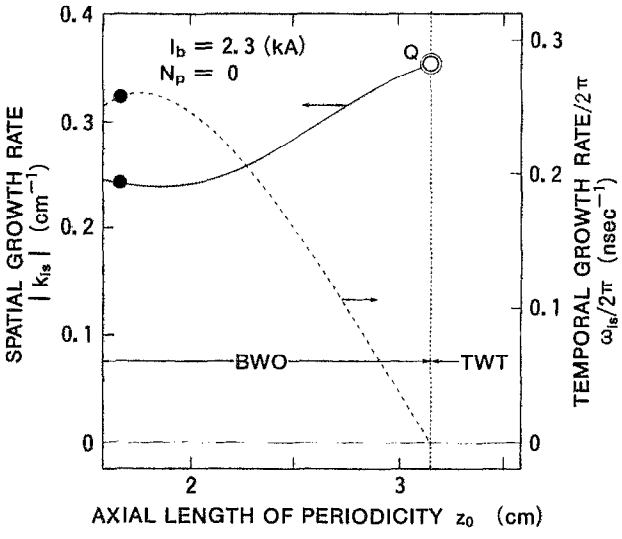

FIG. 5. Spatial growth rate (solid curve) and temporal growth rate (dashed curve) divided by 2π at the saddle point of a vacuum ($N_p = 0$) slow wave structure versus axial length of periodicity, z_0. Other parameters are the same as those in Fig. 4. The solid circles on the curves denote the growth rates corresponding to $z_0 = 1.67$ cm, the experimental value. See the text for the double open circle Q.

circle P of the plasma BWO in Fig. 4(a); this fact suggests that the plasma BWO (Refs. 13 and 14) may be more advantageous than an optimally designed vacuum BWO. The physical explanation of this result obtained in the present analysis is left to be tried in the future.

III. EXCITATION OF A FINITE LENGTH PLASMA-FILLED BWO

So far, we have ignored the end effects of the slow wave structure with finite length L. The analysis of the dispersion relation, $D(k,\omega) = 0$, presented in Sec. II under the assumption L infinity may be extended to the case of finite L structures, provided that L is considerably larger than the average waveguide radius, R_0. The analysis is made in the general framework of the global instability of finite length system shown in the textbook of Lifshitz and Pitaevskii.[19] In other words, we have considered a quasi-steady-state case, where the temporal growth of a wave is considerably smaller than its spatial growth. For systems that are limited in the axial direction, the oscillation is affected by the reflection from both ends. The oscillation in this case should be considered simultaneously as the superposition of an infinite number of waves given by $D(k,\omega) = 0$, i.e., periodic four roots all having identical complex frequency, as is shown in an example in Fig. 1. We have found that, for a given complex ω with large positive ω_i's, three of the four roots (the two beam space charge waves and the forward structure wave) of our $D(k,\omega) = 0$ are located above the separatrix in the complex k plane and having positive group velocities, while a single root (the backward structure wave) is found below the separatrix, where the group velocity is in negative direction, as was explained in the previous section. It is noted here that only one ($k_i < 0$) of the two beam space charge waves with positive group velocities is the source of oscillation that is spatially growing among the four roots, all the rest three roots are either decaying or stable in nature. For a sufficiently long waveguide, we may be able to assume that the spatially growing beam space charge wave, k_+, is only the propagating wave in the positive z direction, provided $|\mathrm{Im}(k_+)L| \gg 1$. It should be noted that the wave k_+ carries the Poynting flux in negative z direction. After reflection from the right end $z = L$, the counterwave, k_-, which propagates in the negative z direction toward $z = 0$, can create a positive feedback in the structure. Because there is only one root, the backward structure wave, k_-, that propagates in the negative z direction, the oscillation in a finite length system will be determined by k_+ and k_-. As is shown in Fig. 6, k_+ (growing wave) and k_- (decaying wave) locate, respectively, above and below the separatrix.

The finite length of the waveguide imposes a new constraint to the choice of a pair of roots, k_+ and k_-. Namely, in the limit of the quasi-steady-state assumption, the condition of coherency that an electromagnetic field at any given point z must be unique imposes the choice of a pair of the roots k_+ and k_- proposed by the following relation given in Eq. (65.4) of Ref. 19: $R_1R_2 \times \exp\{i[k_+(\omega) - k_-(\omega)]L\} = 1$, where R_1 and R_2 are, respectively, the reflection coefficients at $z = 0$ and $z = L$. This is rewritten as follows:

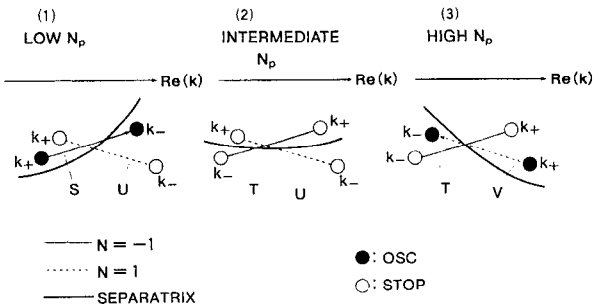

FIG. 6. Schematic drawing of the pair of roots that explain the oscillation and stopping of oscillation in a plasma BWO in (1) low, (2) intermediate, and (3) high plasma densities, respectively. The pair of roots marked by solid and open circles correspond, respectively, to the oscillation and the stopping of oscillation in the plasma BWO.

$$\epsilon = k_- - k_+ = -(2\pi N/L) - i[\ln(R)/L], \quad (3)$$

where $R = |R_1R_2|$ and $N = 0, \pm 1, \pm 2, \ldots$. The arbitrary integer N comes from the fact that an infinite number of sheets of the Riemann surface exist for the complex logarithm function, $\ln(z) = \ln|z| + i[\arg(z) + 2\pi N]$, namely, $\exp(i2\pi N) = 1$. There is a possibility that the structure with length L constitutes a cavity resonator, if $|N|$ and R are comparatively large. For example, if $R = 1$ and $\mathrm{Re}(k_+) = -\mathrm{Re}(k_-)$, $|N|$ becomes the number of half-waves set on the resonator length L. However, we do not consider such a case of a pair of k_+ and k_- with $\mathrm{Re}(k_+) = -\mathrm{Re}(k_-)$ in the present analysis. To facilitate the interpretation of Eq. (3), it may be convenient to imagine Bohr's quantizing condition of atomic states, because they are somewhat analogous in the sense that they require a single valued physical quantity for a given spatial point z and a given time t. Equation (3)must be satisfied for having coherent oscillation from a finite L structure in the quasi-steady-state assumption limit. Unless Eq. (3) is satisfied, oscillation then stays at incoherent, noisy, and low level, no matter how each propagating wave has positive temporal growth rate. In this paper, we define this case as the stopping of oscillation.

The oscillation in a finite length slow wave structure no longer occurs at ω_s and k_s of the saddle point, but at ω and k_+ near the saddle point and are given by Eq. (3) along with the following two equations:

$$D(k_+, \omega) = 0, \quad (4)$$

$$D(k_+ + \epsilon, \omega) = 0. \quad (5)$$

On separating the real and the imaginary parts of ϵ in Eq. (3), we have

$$\mathrm{Re}(\epsilon) = \mathrm{Re}(k_-) - \mathrm{Re}(k_+) = -2\pi N/L, \quad (6)$$

$$\mathrm{Im}(\epsilon) = \mathrm{Im}(k_-) - \mathrm{Im}(k_+) = -\ln(R)/L > 0, \quad (7)$$

where $0 < R < 1$ has been assumed. Equation (7) holds only if $|\mathrm{Im}(k_+)| > |\mathrm{Im}(k_-)|$, because both k_+ and k_- lie in the lower-half k plane, as was shown in Fig. 2. To satisfy Eq. (7), therefore, the global spatial growth rate, defined by $|\mathrm{Im}(k_+)| - |\mathrm{Im}(k_-)|$, must be positive. In other words, the spatial growth rate, $|\mathrm{Im}(k_+)|$, which lies above the separatrix, must surpass the spatial damping rate, $|\mathrm{Im}(k_-)|$,

which lies below the separatrix. The roots k_+ and k_- obtained from Eqs. (3), (4), and (5), therefore, must satisfy the following two conditions simultaneously in order to have coherent oscillation in a finite length structure: (1) positive temporal growth rate, i.e., $\omega_i > 0$; (2) positive global spatial growth rate, i.e., $|\mathrm{Im}(k_+)| - |\mathrm{Im}(k_-)| > 0$. Thus the fact that the reflection coefficient is $0 < R < 1$ imposes an additional restriction for having oscillation. We believe that the following example will give an exact picture of this fact. Equations (3)–(5) are solved simultaneously for the case $N_p = 2 \times 10^{11}\ \mathrm{cm}^{-3}$ and $I_b = 2.3$ kA which are the same as those in Fig. 2, for two different sets of L and R. The pair of roots k, obtained from Eqs. (3)–(5) for $L = 16.7$ cm, $R = 0.1$, and $N = -1$, are marked by solid circles and are denoted by a_+ and a_- in Fig. 2. In this case, the root a_+ above the separatrix is located deeper than the root a_- below the separatrix, i.e., $|\mathrm{Im}(k_+)| > |\mathrm{Im}(k_-)|$, thus the pair of the roots satisfy Eqs. (6) and (7). Moreover, the condition $\omega_i > 0$ is met as shown by the position of a_+. The waveguide with these parameters, therefore, will oscillate. In the case of $L = 28$ cm, $R = 0.02$, and $N = 1$, however, the corresponding pair of the roots are marked by open circles and are denoted by b_+ and b_- in Fig. 2. The root b_+ above the separatrix is located shallower than the root b_- below the separatrix. This fact results in $|\mathrm{Im}(k_+)| < |\mathrm{Im}(k_-)|$. Equation (7), therefore, cannot be satisfied and the structure will no longer oscillate for these parameters, even though the real parts of these roots satisfy Eq. (6) and $\omega_i > 0$, as shown by the position of b_+. It must be noted here that the present analysis is restricted to the case of $N = \pm 1$ only, simply because the solutions are easily found. We cannot find oscillation condition for $N = 0$, because, in this case, $\mathrm{Re}(k_+) = \mathrm{Re}(k_-)$ in Eq. (6), thus k_+ cannot locate below k_-, as is inspected in Fig. 2. However, there may exist possibilities of oscillation for $|N| > 1$.

We have found that the operation of the plasma-filled BWO can be divided into three major cases depending on the filled plasma density, namely, the low, intermediate, and high N_p regions. These are shown schematically in Fig. 6. In vacuum or low N_p case (1), the separatrix is a curve extending from left bottom to right top. For high N_p case (3), the separatrix is from left top to right bottom; and in intermediate values of N_p in case (2), the separatrix is a horizontal curve. For given values of L and R, the pairs of k_+ and k_- satisfying mathematically Eqs. (3)–(5) are connected to each other by solid lines ($N = -1$) and dashed lines ($N = 1$), respectively, in Fig. 6. In (1) low N_p case, the pair of roots for $N = -1$, shown by the solid circles and defined here as the S type of pair, are only found to cause coherent oscillation, as is expected from Eqs. (6) and (7). However, with the increase in N_p, the separatrix gets horizontal and the S type of pair of roots for $N = -1$ changes to T type of pair as shown for (2) intermediate N_p case in Fig. 6. Both pairs of roots for $N = -1$ (T type) and $N = 1$ (U type) are found not to satisfy the conditions for coherent oscillation required by Eqs. (6) and (7) for such N_p's. Further increase in N_p, however, is found to change the U type of pair of roots in the intermediate N_p into V type of pair of roots for $N = 1$ in the case (3) of high N_p. The V type of pair of roots shown by the solid circles for $N = 1$ in the high N_p case (3) are found to cause again coherent oscillation since they satisfy Eqs. (6) and (7). The above discussion reveals that the output radiation from a plasma BWO may stop for an intermediate range of plasma densities.

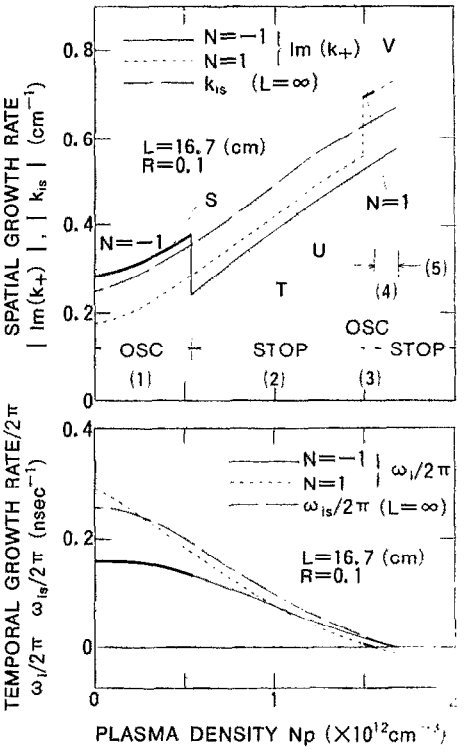

FIG. 7. Growth rates of a finite length plasma-filled corrugated waveguide with $L = 16.7$ cm, $R = 0.1$, and $I_b = 2.3$ kA versus the plasma density N_p. The solid and dashed lines correspond, respectively, to $N = -1$ and $N = 1$. The dot-dashed lines show the growth rates for L infinity. Regions (1) and (3) denoted by OSC (thick solid curves) and those (2), (4), and (5) denoted by STOP correspond, respectively, to the oscillation and stopping oscillation as functions of the plasma density N_p.

The growth rates in $L = 16.7$ cm long plasma-filled corrugated waveguide are shown in Fig. 7. The beam current and the reflection coefficient, R, were held constant at 2.3 kA and 0.1, respectively. The solid and dashed lines are, respectively, for $N = -1$ and $N = 1$. The thicker parts of the curves correspond to coherent oscillation. In the figure, the oscillation in the region (1), due to the S type of pair of roots in Fig. 6, stops in the region (2) where the S type of pair of roots changed into T type of pair of roots in Fig. 6. On the other hand, the oscillation in region (3), due to the V type of pair of roots in Fig. 6, stops in region (2), where the V type of pair of roots changes into U type of pair of roots in Fig. 6. The interception of the oscillation in the regions (2) and (4) are due to the failure in satisfying the condition of positive global spatial growth rate. This novel phenomenon for stopping oscillation in the regions (2) and (4) is caused when the separatrix, shown by thick solid line in Fig. 6, becomes a horizonal curve for such N_p's. In region (5) in Fig. 7, the oscillation is found to stop because of negative ω_i. The growth rates of L infinite structure are also shown by dot-

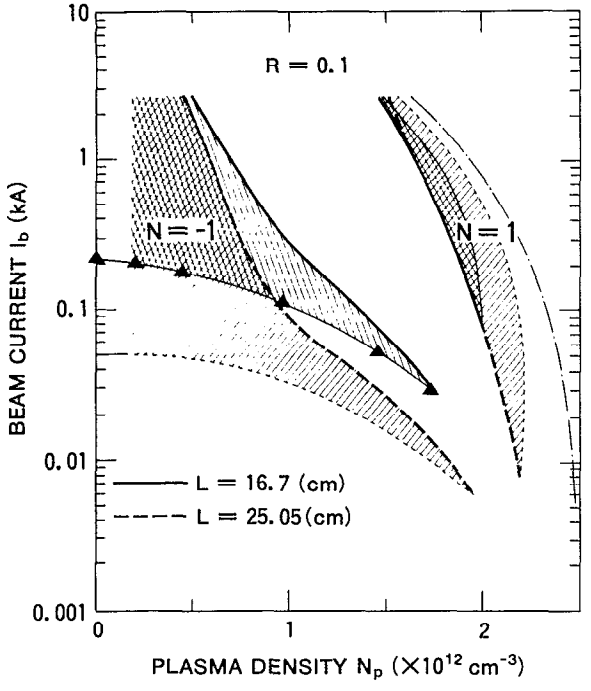

FIG. 8. Hatched oscillation regions in the parameter plane of the beam current, I_b, versus plasma density, N_p. The reflection coefficient $R = 0.1$. The solid and dashed lines correspond, respectively, to waveguides of length $L = 16.7$ and 25.05 cm. The thin dot-dashed curve indicates the maximum plasma density above which the oscillation in an infinitely long waveguide is quenched, because $\omega_{is} < 0$. See the text for solid triangles representing the starting current obtained from three-wave interaction.

dashed lines for comparison. The temporal growth rates for a finite length structure are less than that for L infinite case,[12] as shown in Fig. 7. An opposite situation has occurred, however, for the spatial growth rates.

The oscillation regions are shown by oblilque hatchings in Fig. 8, in a parameter plane of plasma density, N_p, versus the beam current, I_b, for two cases of structure length L. The solid and dashed lines correspond to the cases of $L = 16.7$ and 25.05 cm, respectively. The reflection coefficient R is assumed to be 0.1 and other parameters are the same as those in the previous section. The thinner curves appear from the condition $\omega_i < 0$, while the thicker curves are due to a negative global spatial growth rate. The figure shows that the quenching of the oscillation can occur for an intermediate range of plasma densities. Oscillation happens in two cases, for $N = -1$ in low N_p region and $N = 1$ in high N_p region, as was shown in Fig. 6. The figure also shows that the beam current necessary for the excitation of the plasma BWO, i.e., the starting current, decreases with N_p. The increase in waveguide length is also found to decrease the starting current. The dot-dashed line in Fig. 8 gives a measure of the critical plasma density, determined from the condition $\omega_{is} = 0$, above which the oscillation of TM_{01} mode in an infinitely long waveguide will stop.

Swegle analyzed the starting currents for the oscillation from a vacuum BWO with finite structure length.[12] He calculated the starting current from the condition that $\omega_i = 0$ assuming $R = 0$ in our notation and an annular beam. In the present paper, we assumed a solid beam, and $R = 0$ must be avoided in our formulation, because Eq. (7) becomes infinity. Nevertheless, we have found that our starting currents for $N_p = 0$ are not contradictory to the results by Swegle[12] and by others.[23] Details will be published elsewhere. The main difference is as follows; they sometimes chose $|N| > 1$, whereas we have chosen $N = \pm 1$ in the present paper.

In Fig. 9, the oscillation regions are hatched in a parameter plane of the reflection coefficient, R, versus the waveguide length L. The beam current is $I_b = 2.3$ kA. The solid and dashed lines correspond to the plasma density $N_p = 2\times 10^{11}$ and 1.5×10^{12} cm^{-3}, respectively. The thinner parts of the curves are due to $\omega_i = 0$. The thicker parts of the curves, on the other hand, come from a negative global spatial growth rate. The starting length for oscillation (thinner curves) increases roughly as the reflection coefficient, R, decreases. We observed that the starting length of waveguide filled with plasma for which $N = -1$ (case of $N_p = 2\times 10^{11}$ cm^{-3}) is less than that of a vacuum waveguide. The starting length at N_p's for which $N = 1$ (case of $N_p = 1.5\times 10^{12}$ cm^{-3}) is, however, higher than that of the vacuum case. Over a certain range of the reflection coefficient, R, the waveguide is again found to stop oscillation within an intermediate range of waveguide lengths. The points marked by A and B in this figure correspond, respectively, to the cases for which the roots k obtained from Eqs. (3)–(5) are shown in Fig. 2 by the notations a_+ and b_+.

Finally, Fig. 10 shows the oscillation region by hatching in a parameter plane of reflection coefficient, R, versus the plasma density, N_p, computed under the assumption that I_b

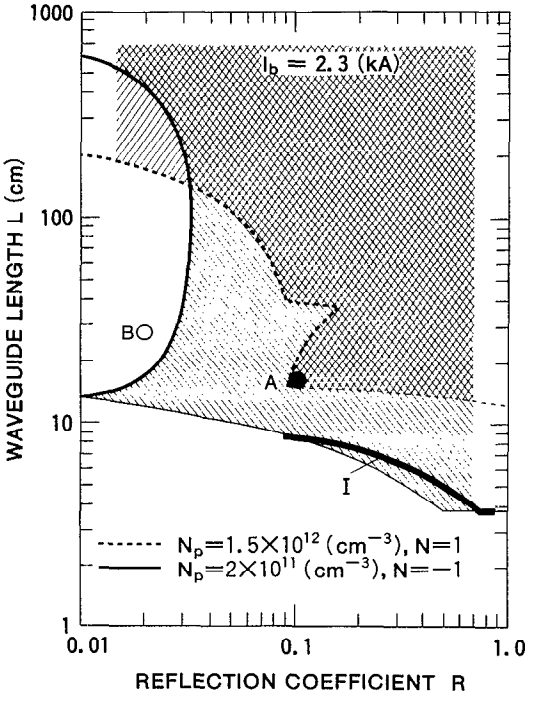

FIG. 9. Hatched oscillation regions in the parameter plane of waveguide length, L, versus reflection coefficient, R, solid and dashed curves are, respectively, for $N_p = 2\times 10^{11}$ and 1.5×10^{12} cm^{-3}; $I_b = 2.3$ kA. See the text for the points A, B, and the thickest solid curve I.

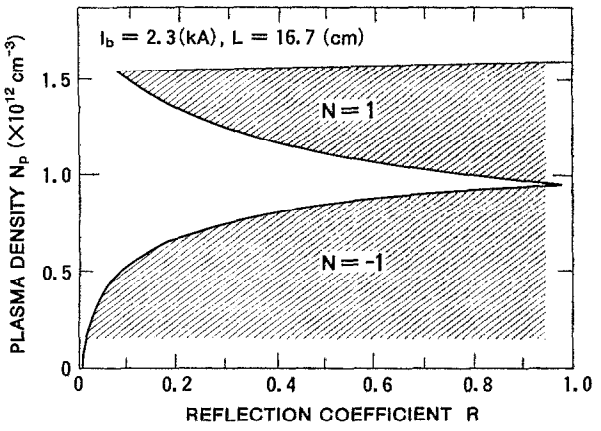

FIG. 10. Hatched oscillation region in the parameter plane of plasma density, N_p, and reflection coefficient, R. $I_b = 2.3$ kA and $L = 16.7$ cm.

$= 2.3$ kA and $L = 16.7$ cm. The temporal growth rate, ω_i, becomes negative when the waveguide is overdriven with plasma above the density determined by the thinner curve, in which case the system becomes plasma TWT. The thicker part of the curve arises from the failure in satisfying the condition of positive global spatial growth rate. Here again, an intermediate range of plasma densities is found to stop oscillation for $R < 0.98$.

IV. DISCUSSION AND CONCLUSIONS

A linear theory for the small signal gain of a plasma-filled backward wave oscillator, driven by an intense relativistic electron beam guided by an infinitely strong axial magnetic field, has been presented assuming a localized source of perturbation. For such a source, the existence of the saddle point with $\omega_{is} > 0$ determines the instability of the infinitely long system. As is well-known, the location of the saddle point can be found by solving the simultaneous equations $D(k,\omega) = 0$ and $\partial D(k,\omega)/\partial k = 0$. Instead of solving these equations, we have devised a convenient numerical technique in the present work to find the locations of the saddle point with sufficient accuracies as much as we want. It is to calculate the finite length waveguide case with exceedingly large L. For L infinity, Eq. (3) yields $k_+ = k_-$, which is nothing but the saddle point. This fact would help us to determine the continuous change in the position of the saddle point over a wide range of plasma density. The results in Figs. 4 and 5 are obtained from Eqs. (3)–(5) with an exceedingly large value of L (8500 cm) and $R = 0.999$ by using the Newton iteration method.[22]

The linear analysis predicts a considerable increase both in the spatial growth rate and in the oscillation frequency with increase in N_p. In general, the relative merits of the spatial and temporal growth rates as a measure of the strength of the instability at linear stage depend on the waveguide length as well as on other experimental conditions. In general, both of the linear growth rates have nothing to do with the radiation output. For example, if the structure length and the time of the development of the instability are both sufficiently large, the output radiation will be determined completely by the nonlinear saturation mechanisms of the system. For a device which is too short to allow the signal to grow up according solely to spatial growth rate, the temporal growth rate at early stage of development could be quite important in determining the output radiation level. Under different circumstances, the spatial growth rate may play a greater role in the development of instability than the temporal growth rate. The saturation levels and efficiencies of plasma-filled BWO's are beyond the scope of the present linear analysis. The enhanced radiation observed in the experiments[13,14] may be related to the linear spatial growth rate which is an increasing function of N_p, rather than the temporal growth rate, a decreasing function of N_p, if the linear process in our analysis was the dominant mechanism for oscillation.

The instability in a finite length plasma-filled slow wave structure has also been analyzed with quasi-steady-state assumption. The four independent periodic roots of fundamental TM_{01} mode shown in Fig. 1 are again depicted schematically for a real frequency f_0 in Fig. 11(a). For the given oscillation frequency, f_0, in Fig. 11(a), E (a_- in Fig. 2) and E' (a'_- in Fig. 2) represent, respectively, the backward and the forward structure waves, and G (a_+ and a''_- in Fig. 2) represents the two beam space charge waves. In Sec. III, we considered a special case of two-wave interaction process between a_+ and a_-, i.e., a mode conversion between the closest modes with $N = \pm 1$ in Eq. (3). In other words, case

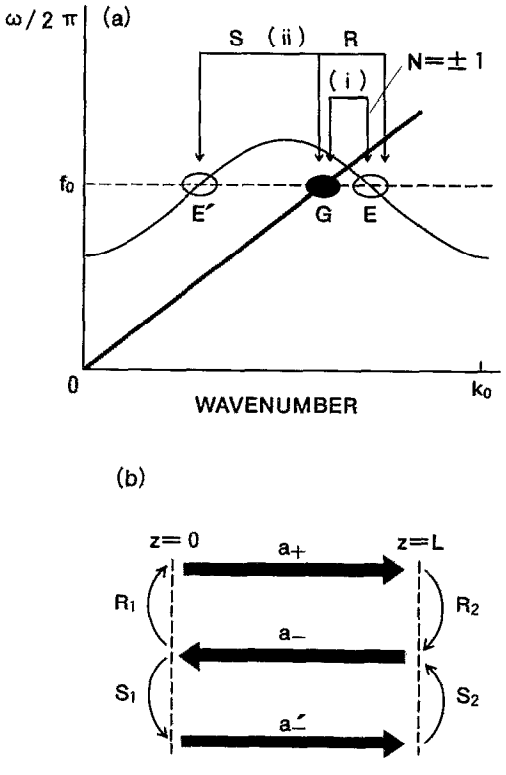

FIG. 11. Explanatory drawing for possible choices of mode conversion due to end reflections: (a) Schematic view of the roots on the dispersion curve; (i) two-wave interaction, (ii) three-wave interaction. (b) A possible model for three-wave interaction.

(i) shown in Fig. 11(a) was considered to analyze the coherent oscillations in a finite length system. This was done on the assumption that the effect of a'_- and a''_- was negligibly small. This will be cleared, if we have a look at the positions of a_+, a_-, a'_-, and a''_- in Fig. 2. All these four roots have an identical complex frequency $\omega/2\pi = (9.075 + i\,0.1553)$ GHz. Positive and negative directions of group velocity are denoted by thick arrows at each root. No doubt, the damping rate of a''_- is the highest regardless to the values of the beam current and can easily be ignored, because it has nothing to do with the resulting oscillation, if $|\mathrm{Im}(k_+)L| \gg 1$. Near the starting current condition for oscillation, however, the damping of a'_- decreases, because it approaches to real k axis ($\omega_i = 0$) in Fig. 2. Accordingly, the effect of a'_- may not be negligible for small beam currents. The validity of the two-wave interaction process for starting current condition is here checked by analyzing a three-wave (a_+, a_-, and a'_-) interaction process, i.e., case (ii) in Fig. 11(a). The mode conversion in the three-wave interaction process is shown schematically in Fig. 11(b). We assume that a_- and a_+ are related to each other by the reflection coefficients R_1 and R_2, respectively, at $z = 0$ and $z = L$. Similarly, a_- and a'_- are assumed to be related to each other by the reflection coefficients S_1 and S_2, respectively, at $z = 0$ and $z = L$. The angular frequency ω and the wave numbers a_+, a_-, and a'_- corresponding to the oscillation of the finite length system can be determined by solving the following equations simultaneously;

$$D(a_+, \omega) = 0,$$
$$D(a_+ + \epsilon, \omega) = 0,$$
$$D(a_+ + \epsilon - \eta, \omega) = 0,$$
$$R\exp(-i\epsilon L) + S\exp(-i\eta L) = 1,$$

where $\epsilon = a_- - a_+$, $\eta = a_- - a'_-$, $R = |R_1R_2|$, and $S = |S_1S_2|$. Assuming $R = S = 0.1$ and $L = 16.7$ cm, we have solved the above equations for various plasma densities to determine the starting beam current for oscillation and the results are shown by the solid triangles in Fig. 8. In this case, the results of the three-wave interaction are not practically different from those of two-wave interaction. The effect of three-wave interaction on the minimum waveguide length necessary to start oscillation has also been checked for $N_p = 2\times 10^{11}$ cm^{-3} with $I_b = 2.3$ kA assuming $R/S = 1$. The result is shown in Fig. 9 by the thickest solid line I. These results show that the term containing S in the last relation of the above equations will be a minor correction, unless S is considerably larger than R. The two-wave interaction process is sufficient in many cases to investigate the oscillation condition of the plasma BWO systems.

In Fig. 8, we obtained the results that oscillation stops for large beam currents, although the system can oscillate for small currents above the starting current. Evidently, the reason for stopping oscillation in high currents here is due to negative global spatial growth rates. This result is somewhat novel and a simple physical explanation cannot be made at this stage of analysis. Here, we just quote a different case of stopping oscillation in a case of exceedingly high-beam currents in vacuum BWO's; for such a current, a large splitting in branches between the fast and slow beam space charge waves in the dispersion relation happens.[9,10] In this Raman regime, the absolute instability can cease to exist, and the oscillation of the fundamental TM_{01} mode may stop resultantly. This example just suggests that stopping of the oscillation for high currents is not very strange physically. The simple and intuitive physical explanation of stopping oscillation for intermediate values of plasma densities, N_p, in Fig. 8 may be as follows. In L infinite case, the beam–structure wave interaction is known to be the strongest in the case of π-mode or 2π-mode oscillation in terms of normalized wave number. These cases correspond, respectively, to the real wave numbers $k_0/2$ and k_0 in our notation. In these cases, the group velocities of the backward structure wave, $|v_g|$, are minimal. These operations have been called EIO's[24] (extended interaction oscillators). The interaction gets strong, when the group velocity of the backward structure wave is small, because of long time of interaction with the beam within the finite length structure. For $N_p = 0$ ($N = -1$) in Fig. 8, our BWO works near π-mode, as was shown in Fig. 4 in Ref. 20. In the case of $I_b = 0$, the dispersion curve in real frequency versus real wave number plane goes upward with increase in N_p, although the undulation of the dispersion curve also decreases. On the other hand, the beam line remains unchanged. The group velocity $|v_g|$ of the backward structure wave at the crossing point with the beam line in that figure may increase accordingly. The the beam–wave interaction may decrease somewhere between π- and 2π-mode operations. Oscillations are still possible, if L or R is sufficiently large, as were shown in Figs. 9 and 10. For small L or R, however, the system may no longer maintain coherent oscillation, resulting in the intermission of BWO, as was shown in Fig. 8. For a large N_p ($N = 1$), the BWO may recover again, because the interaction approaches 2π-mode. In the case of nonzero I_b also, similar situation to the case of $I_b = 0$ may happen. Increase in the group velocity is estimated as follows. The intermission of the BWO occurred, when the separatrix becomes a horizontal curve, as was shown in case (2) in Fig. 6. The group velocity $|v_g| = |\partial\omega_r/\partial k_r| = |\partial\omega_i/\partial k_i| \doteqdot |\Delta\omega_i/\Delta k_i|$, as was given by Eq. (2.6.8) in Ref. 25 or equivalently by Cauchy–Riemann relationship for a complex function $\omega = f(k)$. When the separatrix near the saddle point in complex k plane is horizontal, $|\Delta k_i|$ must be small for a given $\Delta\omega_i$, i.e., an amount of approach to real axis in complex ω plane keeping ω_r constant. This is because the solid arrow lines in Fig. 2 must be parallel to the separatrix near the saddle point. Accordingly, $|v_g|$ is large, and beam–structure wave interaction becomes weak. We cannot find the pair of k_+ and k_- for coherent oscillation, as was shown in case (2) in Fig. 6, if L or R is small. On the other hand, for low N_p or high N_p case, $|v_g|$ is small because of increased $|\Delta k_i|$, and we may have a possibility to find appropriate pair of k_+ and k_- for coherent oscillation which satisfy Eqs. (3)–(7), even if L or R is small.

In conclusion, in finite length plasma-filled BWO's, we have found that there are two reasons that can prevent $N = \pm 1$ oscillation; (1) the negative temporal growth rates, and (2) the negative global spatial growth rates. The second condition comes from the requirement that the spa-

tial growth rate of the beam space-charge wave must be greater than the spatial damping rate of the backward structure wave for effective positive feedback, because the waveguide is leaky, i.e., $0 < R < 1$. As a result of the second condition, coherent oscillation in the plasma-filled BWO's stops for intermediate ranges of plasma density, beam current, and even for structure length.

ACKNOWLEDGMENTS

The authors would like to acknowledge profoundly the invaluable discussions with Dr. Y. Carmel, Dr. B. Levush, and Dr. T. M. Antonsen, Jr., University of Maryland; Dr. R. A. Kehs, Harry Diamond Laboratories; and Dr. J. A. Swegle, Lawrence Livermore National Laboratory. Valuable comments on EIO's by T. Okamoto, Toshiba Company, Japan, are gratefully acknowledged. Thanks are also due to T. Hosokawa, S. Amano, and T. Nomura, Niigata University, Japan, for their assistance in computer operation.

This work is partly supported by a cooperative research program, National Institute for Fusion Science, Japan.

[1] V. L. Granatstein and I. Alexeff, *High-Power Microwave Sources* (Artech House, Boston, 1987).
[2] Y. Carmel, J. Ivers, R. E. Kribel, and J. Nation, Phys. Rev. Lett. **33**, 1278 (1974).
[3] Yu. V. Tkach, Ya. B. Fainberg, I. I. Magda, N. I. Gaponenko, G. V. Skachek, S. S. Pushkarev, N. P. Gadetskii, and A. A. Belukha, Fiz. Plazmy **1**, 81 (1975) [Sov. J. Plasma Phys. **1**, 43 (1975)].
[4] Yu. V. Tkach, N. P. Gadetskii, Yu. P. Bliokh, E. A. Lemberg, M. G. Lyubarskii, V. V. Ermolenko, V. V. Dyatlova, S. I. Naisteter, I. I. Magda, S. S. Pushkarev, and G. V. Skachek, Fiz. Plazmy **5**, 1012 (1979) [Sov. J. Plasma Phys. **5**, 566 (1979)].
[5] L. S. Bogdankevich, M. V. Kuzelev, and A. A. Rukhadze, Zh. Tekh. Fiz. **50**, 233 (1980) [Sov. Phys. Tech. Phys. **25**, 143 (1980)].
[6] A. S. El'chaninov, F. Ya. Zagulov, N. F. Kovalev, S. D. Korovin, N. V. Rostov, and A. V. Smorgonskii, Pis'ma Zh. Tekh. Fiz. **6**, 443 (1980) [Sov. Tech. Phys. Lett. **6**, 191 (1980)].
[7] V. I. Kurilko, V. I. Kucherov, and A. O. Ostrovskii, Zh. Tekh. Fiz. **51**, 1415 (1981) [Sov. Phys. Tech. Phys. **26**, 812 (1981)].
[8] Y. Carmel, V. L. Granatstein, and A. Gover, Phys. Rev. Lett. **51**, 566 (1983).
[9] J. A. Swegle, J. W. Poukey, and G. T. Leifeste, Phys. Fluids **28**, 2882 (1985).
[10] J. A. Swegle, Phys. Fluids **28**, 3696 (1985).
[11] R. A. Kehs, A. Bromborsky, B. G. Ruth, S. E. Graybill, W. W. Destler, Y. Carmel, and M. C. Wang, IEEE Trans. Plasma Sci. **PS-13**, 559 (1985).
[12] J. A. Swegle, Phys. Fluids **30**, 1201 (1987).
[13] K. Minami, W. R. Lou, W. W. Destler, R. A. Kehs, V. L. Granatstein, and Y. Carmel, Appl. Phys. Lett. **53**, 559 (1988).
[14] Y. Carmel, K. Minami, R. A. Kehs, W. W. Destler, V. L. Granatstein, D. Abe, and W. L. Lou, Phys. Rev. Lett. **62**, 2389 (1989).
[15] S. P. Bugaev, V. A. Cherepenin, V. I. Kanavets, A. I. Klimov, A. D. Kopenkin, V. I. Koshelev, V. A. Popov, and A. I. Slepkov, IEEE Trans. Plasma Sci. **PS-18**, 525 (1990).
[16] S. P. Bugaev, V. A. Cherepenin, V. I. Kanavets, V. I. Koshelev, V. A. Popov, and A. N. Vlasov, IEEE Trans. Plasma Sci. **PS-18**, 518 (1990).
[17] A. T. Lin and L. Chen, Phys. Rev. Lett. **63**, 2808 (1989).
[18] R. J. Briggs, *Electron-Stream Interaction with Plasmas* (MIT Press, Cambridge, MA, 1964), Chap. 2.
[19] E. M. Lifshitz and L. P. Pitaevskii, *Physical Kinetics* (Pergamon, New York, 1981), p. 282.
[20] K. Minami, Y. Carmel, V. L. Granatstein, W. W. Destler, W. R. Lou, D. K. Abe, R. A. Kehs, M. M. Ali, T. Hosokawa, K. Ogura, and T. Watanabe, IEEE Trans. Plasma Sci. **PS-18**, 537 (1990).
[21] M. M. Ali, K. Minami, K. Ogura, T. Hosokawa, H. Kazama, T. Ozawa, T. Watanabe, Y. Carmel, V. L. Granatstein, W. W. Destler, R. A. Kehs, W. R. Lou, and D. Abe, Phys. Rev. Lett. **65**, 855 (1990).
[22] Details of the generalized schemes will be published elsewhere.
[23] B. Levush and T. M. Antonsen, Jr., Proceedings of the International Conference on Plasma Science, 1990, p. 135.
[24] D. H. Preist and W. J. Leidigh, IEEE Trans. Electron Devices **ED-10**, 201 (1963).
[25] A. F. Alexandrov, L. S. Bogdankevich, and A. A. Rukhadze, *Principle of Plasma Electrodynamics* (Springer-Verlag, New York, 1984), p. 34.